15th Triennial World Congress, Barcelona, Spain

THE USE OF MULTIPLE ACTUATORS IN THE ROBUST CONTROL OF AN ACOUSTIC DUCT ⋆

Ian R. Petersen, Himanshu R. Pota and M. Reza Sayyah Jahromi *

* *School of Electrical Engineering, University of New South Wales at the Australian Defence Force Academy, Campbell, ACT 2600, Australia, Phone +61 2 62688446, FAX +61 2 62688443, email: irp@ee.adfa.oz.au*

Abstract: The paper considers the problem of robust active noise control in an acoustic duct. In particular, the paper considers how the number of actuator speakers affects the performance of the system. The robust controller design methodology being considered is based on some recent results on minimax LQG control. The paper also uses a structured approach to uncertainty modelling as part of the controller design scheme.

Keywords: Active Noise Control, Robust control, Minimax LQG control, Uncertainty modelling, Multiple Actuators.

1. INTRODUCTION

The problem of robust feedback control in an acoustic duct has attracted considerable research interest. Acoustic ducts have a number of characteristics which make it difficult to design high performance feedback controllers and it has been found that only limited amounts of noise disturbance attenuation can be achieved via the use of single-input single-output robust feedback controllers; e.g., see (Petersen and Pota, 2000). The aim of this paper is to determine if the use of multiple actuator speakers can significantly improve the performance of robust feedback control systems in this application. We propose an uncertainty model such that the addition of extra actuators does not reduce the achieved performance. This is an important issue in any robust control problem since the addition of an extra actuator will require the addition of extra uncertainty in the uncertain system model. Thus, if the uncertain system modelling technique is overly conservative, the addition of this extra uncertainty may outweigh the benefit if the extra control input and poorer control system performance may result.

Our results are based on an experimental acoustic duct available at the Australian Defence Force Academy (ADFA). The experimental duct available has highly complicated dynamics which are not easily modelled via a theoretical analysis. Thus, the basis of our nominal modelling process will be the use of system identification techniques. In our case, the experimental data consists of frequency response data measured using a swept sine spectrum analyzer.

Our feedback control system design relies on a recent robust controller synthesis technique referred to as minimax LQG control; e.g., see (Petersen *et al.*, 2000; Ugrinovskii and Petersen, 1998) for complete details of this technique. This technique begins with an uncertain system model of the process to be controlled and then constructs an output feedback controller which minimizes the worst case of a quadratic cost function when the system is assumed to be subject to a white noise disturbance. In order to obtain an uncertain system model to which the minimax LQG controller synthesis technique can be applied, we characterize the size of the uncertainty as a function of frequency. Frequency weighting filters are designed to match the magnitude of the error frequency responses. Our approach to constructing these weighting filters applies a Yule-Walker filter design method to the error

⋆ This work was supported by the Australian Research Council.

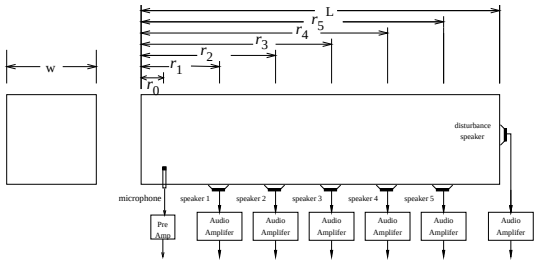

Fig. 1. Acoustic Duct.

frequency response data; e.g., see (Friedlander and Porat, 1984). This method is applied to each actuator channel and then the overall uncertain system model is obtained by combining these uncertain system models together with appropriate scaling parameters.

We also include some analysis to derive limits on the achievable disturbance attenuation.

2. EXPERIMENTAL SETUP AND MODELING

2.1 *Experimental Setup*

The experimental acoustic duct to be considered in this paper is illustrated in Figure 1. This is a duct with a square cross section which is closed at both ends. A microphone is located at position r_0 and control speakers 1–5 are positioned at $r_1 - r_5$ respectively. Also, a disturbance speaker is located at one end of the duct. This speaker is labelled speaker 6. The length of the duct is L. For the experimental duct located at ADFA, the dimensions are as follows: $L = 4.01$m, $w = 0.38$m, $r_0 = 0.19$m, $r_1 = 0.80$m, $r_2 = 1.41$m, $r_3 = 2.19$m, $r_4 = 2.80$m, and $r_5 = 3.41$m.

2.2 *System Identification and Nominal Modeling*

The nominal model used in our robust control system design is obtained by a process of system identification applied to experimental frequency response data measured using a spectrum analyser. In our system identification procedure, the method of (McKelvey *et al.*, 1996) was applied to estimate a 20th order, six-input, single-output state space model whose inputs correspond to the disturbance speaker and each of the control speakers. However, a given controller may not use all of the control input speakers.

The identified model was based on the corresponding frequency response data over the frequency range $10 - 250$ Hz. Also, the parameter q in the algorithm described (McKelvey *et al.*, 1996) was set at $q = 50$. Figure 2 shows the nominal model obtained and the measured magnitude frequency responses for each of the five control speakers. Using this approach nominal modelling, we end up with an nominal transfer function matrix of the form $P(s) = \begin{bmatrix} P_1(s) & P_2(s) \end{bmatrix}$ where $P_1(s)$ represents the transfer function from the disturbance speaker input to the microphone output and

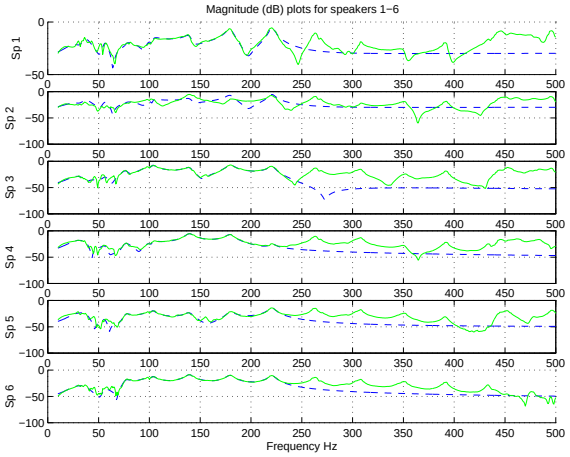

Fig. 2. Model (dashed) and measured (solid) duct frequency responses.

$P_2(s)$ represents the transfer function matrix from the control speaker inputs to the microphone output. Let k denote the number of actuator speakers being used. Then, $P_2(s)$ will be a $1 \times k$ transfer function.

2.3 *Uncertainty Modeling*

The minimax LQG approach which will be used in our controller design begins with an uncertain system model. In order to obtain an uncertain system which is compatible with the minimax LQG control theory, the uncertainty will be represented by frequency weighted uncertainty as shown in Figure 3.

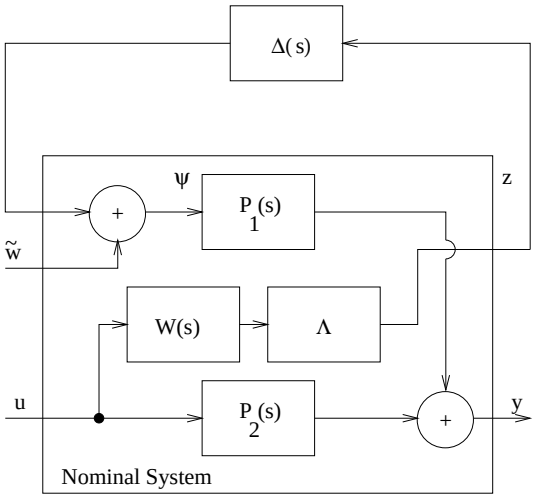

Fig. 3. Uncertain system representation.

In this uncertain system, $\tilde{w}$ represents the disturbance input, $\Delta(s)$ is a $1 \times k$ stable uncertain transfer function matrix subject to the bound

$$\|\Delta(j\omega)\| \leq 1 \ \forall \ \omega. \qquad (1)$$

Also, $W(s) = \begin{bmatrix} W_1(s) & 0 & \dots 0 \\ 0 & W_2(s) & \\ \vdots & & \ddots \ \vdots \\ 0 & \dots & W_k(s) \end{bmatrix}$, is a diagonal matrix of frequency weighting transfer func-

tions which describes the size of the uncertainty in the corresponding speaker channel as a function of frequency. The diagonal matrix

$$\Lambda = \begin{bmatrix} \lambda_1 & 0 & \dots 0 \\ 0 & \lambda_2 & \\ \vdots & & \ddots \quad \vdots \\ 0 & \dots & \lambda_k \end{bmatrix}$$

is a matrix of scaling parameters in the uncertain system model which will be chosen as part of the minimax LQG controller synthesis. The signal u is the control input, and y is the measured output. This uncertain system will be constructed in order to represent the uncertainty in the transfer functions from the control input speakers to the microphone output. The true transfer function matrix from the control input speakers to the microphone output is assumed to be

$$\tilde{P}_2(s) = P_2(s) + P_1(s)\Delta(s)W(s)\Lambda. \tag{2}$$

To construct $W(s)$, we choose each $W_i(s)$ so that

$$\left| \frac{\tilde{P}_{2i}(j\omega) - P_{2i}(j\omega)}{P_1(j\omega)W_i(j\omega)} \right| \leq 1 \; \forall \omega \tag{3}$$

where $P_{2i}(s)$ is the ith component of the nominal transfer function matrix $P_2(s)$. Also, it follows from (2) that $\Delta_i(s)$, the ith component of the uncertain transfer function matrix $\Delta(s)$ satisfies

$$\Delta_i(s) = \frac{\tilde{P}_{2i}(j\omega) - P_{2i}(j\omega)}{P_1(j\omega)W_i(j\omega)\lambda_i}.$$

Thus, it follows from (3) that the condition (1) will be satisfied if Λ is such that

$$\sum_{i=1}^{k} \frac{1}{\lambda_i^2} \leq 1. \tag{4}$$

In practice, we choose Λ so that equality holds in this constraint and thus

$$\lambda_k = \left[1 - \sum_{i=1}^{k-1} \frac{1}{\lambda_i^2} \right]^{-\frac{1}{2}}. \tag{5}$$

Thus, we choose the weighting transfer function $W(s)$ so that (3) holds when $\tilde{P}_2(j\omega)$ is the measured frequency matrix response from the control input speakers to the microphone output and $P_1(j\omega)$ and $P_2(j\omega)$ are the model frequency responses. Also, we choose the scaling constants $\lambda_1 \dots \lambda_{k-1}$ so that

$$\sum_{i=1}^{k-1} \frac{1}{\lambda_i^2} \leq 1. \tag{6}$$

Then λ_k is defined by (5). The parameters $\lambda_1 \dots \lambda_{k-1}$ will then be chosen as part of the minimax LQG procedure described below.

In order to construct a suitable weighting transfer functions $W_i(s)$ to (approximately) satisfy (3), we will use a version of the Yule-Walker filter design algorithm; see (Friedlander and Porat, 1984). In particular, we require that the magnitude frequency response of $W_i(s)$ approximates the function

$$\Phi_i(j\omega) \triangleq \left| \frac{\tilde{P}_{2i}(j\omega) - P_{2i}(j\omega)}{P_1(j\omega)} \right| \tag{7}$$

over the frequency range $[\omega_0, \omega_c]$ for which the nominal model attempts to match the measured data. Above the cutoff frequency ω_c (chosen to be 270 Hz in our case), the nominal model makes no attempt to match the measured frequency response data so we simply require the magnitude of $W_i(j\omega)$ approximates a constant value equal to $\Phi(j\omega_c)$.

For each value of i, we used the above Yule-Walker method to construct a corresponding weighting transfer function $W_i(s)$ of order 16. Plots of the functions $|\Phi_i(j\omega)|$ and $|W_i(j\omega)|$ are shown in Figure 4.

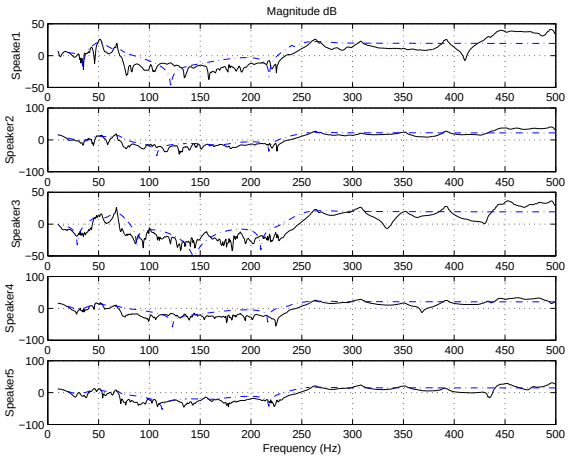

Fig. 4. Frequency response of $|W_i(j\omega)|$ (dashed) and $|\Phi_i(j\omega)|$ (solid).

3. MINIMAX LQG CONTROL

In this section, present a brief description of the minimax LQG robust controller synthesis method. A more complete and rigorous description of this method can be found in the references (Ugrinovskii and Petersen, 1998; Petersen *et al.*, 2000). The minimax LQG method is applied to a stochastic uncertain system of the form shown in Figure 5.

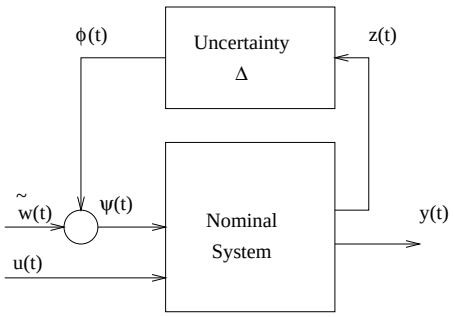

Fig. 5. Stochastic uncertain system.

In this figure, the nominal system is described by the following stochastic state equations:

$$\begin{aligned}\dot{x} &= (Ax + B_1 u + B_2\phi)dt + B_2\tilde{w},\\ z &= C_1 x + D_1 u,\\ y &= (C_2 x + D_2\phi)dt + D_2\tilde{w}.\end{aligned} \tag{8}$$

In the above equations, $x(t) \in \mathbf{R}^n$ is the state, $u(t) \in \mathbf{R}^m$ is the control input, $\tilde{w}(t)$ is a unity covariance white noise input, $z(t) \in \mathbf{R}^q$ is the uncertainty output, $\phi(t) \in \mathbf{R}^p$ is the uncertainty input and $y(t) \in \mathbf{R}^l$ is the measured output.

The uncertainty block can be any dynamical system such that the following stochastic uncertainty constraint is satisfied:

$$\lim_{T\to\infty} \frac{1}{T}\mathbf{E}\left[\int_0^T \|\phi\|^2 dt - \int_0^T \|z\|^2 dt\right] \leq 0. \tag{9}$$

In particular, this stochastic uncertainty constraint will be satisfied if the uncertainty block is a stable linear time invariant system with transfer function matrix $\Delta(s)$ satisfying $\|\Delta(j\omega)\| \leq 1 \quad \forall \quad \omega$. Thus the duct uncertain system described as in Figure 3 and equation (1) will fit into this framework.

It is assumed that the cost function under consideration is of the form

$$J = \lim_{T\to\infty} \frac{1}{2T}\mathbf{E}\int_0^T (x(t)'Rx(t) + u(t)'Gu(t))dt, \tag{10}$$

where $R \geq 0$ and $G > 0$. The minimax LQG control problem involves finding a controller which minimizes the maximum of this cost function where the maximum is taken over all uncertainties satisfying the stochastic uncertainty constraint (9).

If we define a variable

$$\zeta = \begin{bmatrix} R^{\frac{1}{2}}x \\ G^{\frac{1}{2}}u \end{bmatrix}, \tag{11}$$

the cost function (10) can be rewritten as $J = \lim_{T\to\infty} \frac{1}{T}\mathbf{E}\int_0^T \|\zeta\|^2 dt$. The minimax LQG control problem can now be solved by solving the scaled H^∞ control problem represented in Figure 6. In this

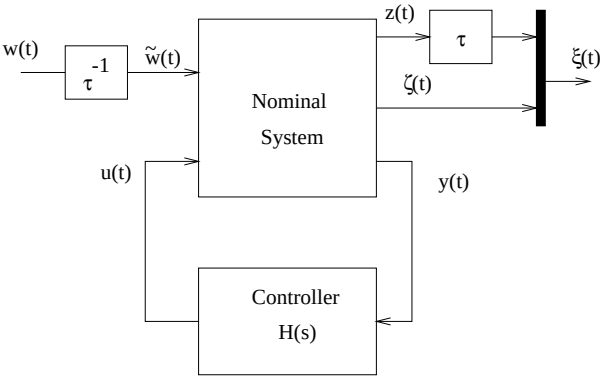

Fig. 6. The scaled H^∞ control problem.

H^∞ control problem, the nominal system is described by equations (8) and (11) and the controller is to be constructed such that the closed loop system is stable and the transfer function from $\tilde{w}(t)$ to $\xi(t)$ satisfies the H^∞ norm bound $\|T_{\tilde{w}\xi}(j\omega)\| \leq 1 \quad \forall\omega$. It is well known that the solution to this H^∞ control problem can be obtained in terms of the following pair algebraic Riccati equations (e.g., see (Zhou *et al.*, 1996)):

$$\begin{aligned}&(A - B_2D_2'(D_2D_2')^{-1}C_2)Y_\infty\\ &+Y_\infty(A - B_2D_2'(D_2D_2')^{-1}C_2)'\\ &-Y_\infty(C_2'(D_2D_2')^{-1}C_2 - \frac{1}{\tau}R_\tau)Y_\infty\\ &+B_2(I - D_2'(D_2D_2')^{-1}D_2)B_2' = 0\end{aligned} \tag{12}$$

and

$$\begin{aligned}&X_\infty(A - B_1G_\tau^{-1}\Upsilon_\tau') + (A - B_1G_\tau^{-1}\Upsilon_\tau')'X_\infty\\ &+(R_\tau - \Upsilon_\tau G_\tau^{-1}\Upsilon_\tau')\\ &-X_\infty(B_1G_\tau^{-1}B_1' - \frac{1}{\tau}B_2B_2')X_\infty = 0,\end{aligned} \tag{13}$$

where the solutions are required to satisfy the conditions $Y_\infty > 0$, $X_\infty > 0$, $I - \frac{1}{\tau}Y_\infty X_\infty > 0$ and $R_\tau - \Upsilon_\tau' G_\tau^{-1}\Upsilon_\tau \geq 0$. Here $R_\tau \triangleq R + \tau C_1'C_1$, $G_\tau \triangleq G + \tau D_1'D_1$ and $\Upsilon_\tau \triangleq \tau C_1'D_1$. In order to solve the minimax LQG control problem, the parameter $\tau > 0$ is chosen to minimize the cost bound W_τ defined by

$$W_\tau \triangleq \text{tr}\begin{bmatrix} (\tau YC_2^T + B_2D_2^T)(D_2D_2^T)^{-1} \\ \times(\tau C_2Y + D_2B_2^T)X(I - YX)^{-1} \\ +\tau YR_\tau \end{bmatrix}. \tag{14}$$

Then, the minimax LQG controller is defined by the state equations

$$\begin{aligned}\dot{\hat{x}} &= (A - B_1G_\tau^{-1}\Upsilon_\tau')\hat{x}\\ &\quad -(B_1G_\tau^{-1}B_1' - \frac{1}{\tau}B_2B_2')X_\infty)\hat{x}\\ &\quad +(I - \frac{1}{\tau}Y_\infty X_\infty)^{-1}(Y_\infty C_2' + B_2D_2')\\ &\quad \times(D_2D_2')^{-1}\left(y - (C_2 + \frac{1}{\tau}D_2B_2'X_\infty)\hat{x}\right)\\ u_\tau &= -G_\tau^{-1}(B_1'X_\infty + \Upsilon_\tau')\hat{x}.\end{aligned} \tag{15}$$

4. CONTROLLER DESIGN

In order to apply the minimax LQG technique described in Section 3, we must first specify the stochastic uncertain system (8), (9) and the cost function (10). The uncertain system to be considered is derived from the block diagram shown in Figure 3 where the transfer function matrices $P_1(s)$, $P_2(s)$ and $W(s)$ are defined as above. This defines a corresponding stochastic uncertain system of the form (8), (9). In this stochastic uncertain system, the state equations (8) are obtained from a state space realization of the transfer function $P(s)$ augmented with the transfer function matrix $W(s)\Lambda$ as in Figure 3. Also, the condition (1) guarantees the satisfaction of the stochastic uncertainty constraint (9).

We choose the matrix R in the cost function (10) as $R = C_2'C_2$. That is, the term $x(t)'Rx(t)$ in the cost function (10) corresponds to the norm squared value of the nominal system output. The term $u'Gu$ in the cost function (10) is treated as a design parameter affecting controller gain. However, in all cases it was found that setting G to the small value of $G = 10^{-8}$ did not lead to excessive controller gains.

The minimax LQG controller is synthesized by first choosing the constant $\tau > 0$ and the parameters λ_i to minimize the quantity W_τ defined in (14). This optimization was carried out using the matlab unconstrained optimization command **fminsearch**. With the optimal value of the parameter τ and the matrix Λ, the controller is constructed according to the formula (15). The order of this controller will be $20 + 16k$ where k is the number of control speakers being used. Such a high order controller may lead to implementationproblems. Hence, the balanced controller reduction method described in Section 19.1.1 of (Zhou *et al.*, 1996) was applied in order to obtain a 15th order approximation to the original controller. The controller design methodology described above was applied to the cases of $k = 1, 2, \ldots, 5$ control speakers.

5. EXPERIMENTAL RESULTS

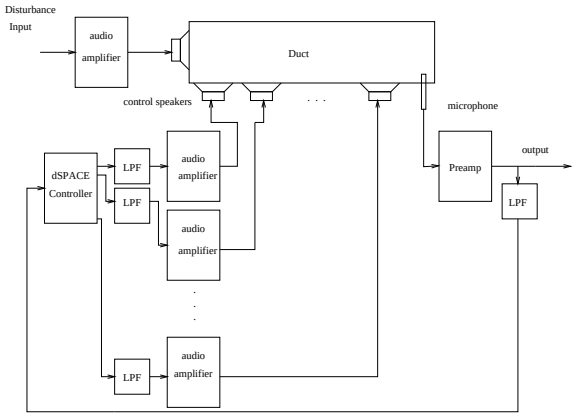

Fig. 7. Feedback controller setup.

Each of the controllers designed in Section 4 were implemented on a dSPACE DEC alpha system as shown in Figure 7. This involved first discretizing the reduced dimension controller using the FOH method with a sample period of 0.5×10^{-3} seconds. The resulting discrete time controller was then implemented on the dSPACE system with this sample period. Figures 8-9 show the resulting experimental frequency responses for each of the corresponding closed loop systems. These figures also show the measured frequency response for the uncontrolled duct.

The measured disturbance attenuation over the range of 10 to 250 Hz together with the optimal value of the cost bound W_τ for each of the cases being considered is shown in Table 1. From Figures 8-9 and Table 1, we can see that some improvement is obtained in the

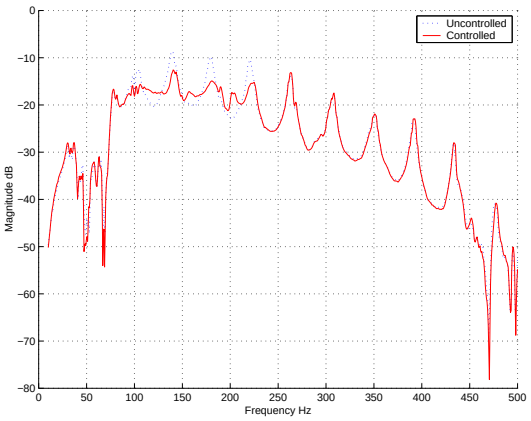

(a) Control using Speaker 1

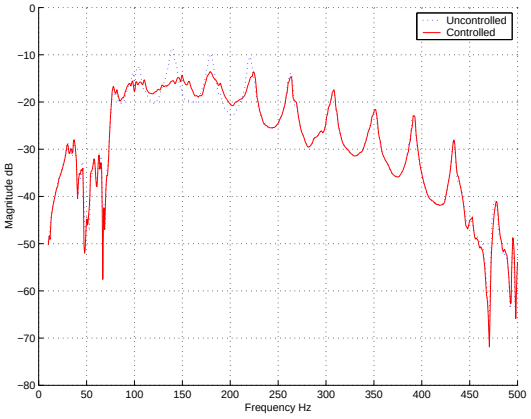

(b) Control using Speakers 1-2

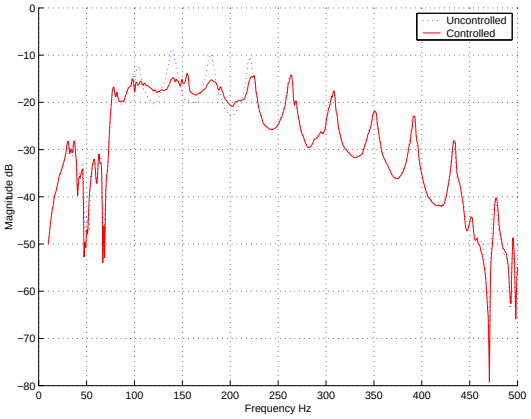

(c) Control using Speakers 1-3

Fig. 8. Experimental controlled and uncontrolled frequency responses.

control system performance as the number of control speakers is increased from 1 to 3. However, increasing the number of speakers beyond 3 does not result in a significant increase in performance.

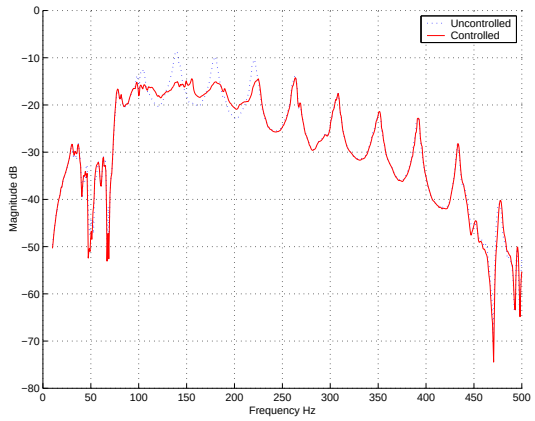

(a) Control using Speakers 1-4

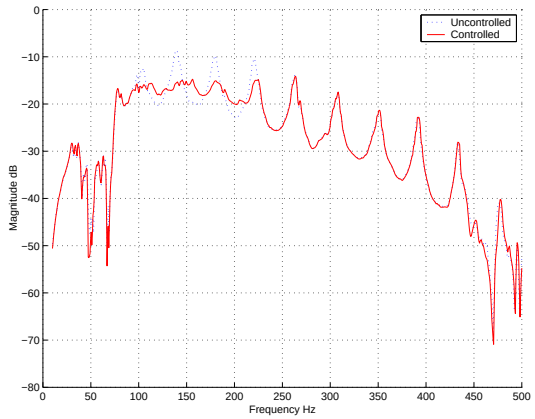

(b) Control using Speakers 1-5

Fig. 9. Experimental controlled and uncontrolled frequency responses.

Number of Control Speakers	Measured attenuation	W_τ
1	3.8 dB	3.78
2	4.4 dB	3.64
3	5.1 dB	3.56
4	5.2 dB	3.58
5	5.3 dB	3.64

Table 1. Measured disturbance attenuation and LQG cost bounds.

6. PERFORMANCE LIMITATIONS

The experimental closed loop frequency responses obtained in the previous section lead us to the question of what are the limits on the achievable noise attenuation. We now present a rule of thumb which gives the performance limitations due to unmodelled dynamics in terms of modal density. In this rule of thumb, we ignore the effect of non-minimum phase zeros. The presence of non-minimum phase zeros would impose even more severe limitations.

First note that the closed loop transfer for the duct control system will be given by the formula $P_{cl}(s) = \frac{\tilde{P}_1(s)}{1+L(s)}$. where $L(s)$ is the scalar loop gain $L(s) = -\tilde{P}_2(s)H(s)$ and $H(s)$ is the controller transfer function matrix. Suppose that $\tilde{P}_1(s)$ has a resonant peak at ω_1 which we wish to attenuate. Also, suppose $\tilde{P}_2(s)$ has an unmodelled resonance at $\omega_2 > \omega_1$ and hence the phase of the loop gain $L(s)$ is unknown at ω_2. Hence, to guarantee closed loop stability, we must ensure $20\log_{10}|L(j\omega_2)| \leq 0 \quad dB$. To achieve disturbance attenuation of α at ω_1, we must have $\frac{1}{|1+L(j\omega_1)|} = \alpha$. This can be approximated by $20\log_{10}|L(j\omega_1)| \approx 20\log_{10}\left(\frac{1}{\alpha}-1\right)$. For $\alpha < 0.5$, this means that $L(s)$ must have gain crossover frequency between ω_1 and ω_2. Thus, at the gain crossover frequency, the average roll-off slope of the gain bode plot of $L(s)$ is bounded below by $\frac{20\log_{10}\left(\frac{1}{\alpha}-1\right)}{20\log_{10}\frac{\omega_2}{\omega_1}}$ dB/decade. Using the approximate version of Bode's Gain Phase relation and assuming $L(s)$ is minimum phase, this slope must be bounded as follows to achieve closed loop stability: $\frac{20\log_{10}\left(\frac{1}{\alpha}-1\right)}{20\log_{10}\frac{\omega_2}{\omega_1}} \leq 40$ dB/decade. This is equivalent to

$$-20\log_{10}\alpha \leq 20\log_{10}\left(1+\frac{\omega_2^2}{\omega_1^2}\right) \quad dB. \qquad (16)$$

This is our rule of thumb indicating a bound on the achievable disturbance attenuation in terms of the final modal density ω_2^2/ω_1^2. For the duct resonance at 220Hz, this formula gives a bound of 7.7 dB compared with the 3.3 dB reduction of this peak we obtained in the case of the all five control speakers.

7. REFERENCES

Friedlander, B. and B. Porat (1984). The modified Yule-Walker method of ARMA spectral estimation. *IEEE Transactions on Aerospace Electronic Systems* **20**(2), 158–173.

McKelvey, T., H. Akçay and L. Ljung (1996). Subspace-based multivariable system identification from frequency response data. *IEEE Transactions on Automatic Control* **41**(7), 960–979.

Petersen, I. R. and H. R. Pota (2000). Minimax LQG control of an experimental acoustic duct. In: *IEE Control 2000 Conference*. Cambridge UK.

Petersen, I. R., V. Ugrinovski and A. V. Savkin (2000). *Robust Control Design using H^∞ Methods*. Springer-Verlag London.

Ugrinovskii, V. A. and I. R. Petersen (1998). Time-averaged robust control of stochastic partially observed uncertain systems. In: *Proceedings of the IEEE Conference on Decision and Control*. Tampa, FL.

Zhou, K., J. Doyle and K. Glover (1996). *Robust and Optimal Control*. Prentice-Hall. Upper Saddle River, NJ.